

Electronic Supplementary Information

Chiral Smectic Phase Induced by Alternating External Field

Zi-Qin Chen,^{†,‡} Yu-Wei Sun,^{†,‡} You-Liang Zhu,^{†,‡} Zhan-Wei Li,^{*,†,‡} and Zhao-Yan
Sun^{*,†,‡}

*State Key Laboratory of Polymer Physics and Chemistry, Changchun Institute of Applied
Chemistry, Chinese Academy of Sciences, Changchun 130022, China, and University of Science
and Technology of China, Hefei, 230026, China*

E-mail: zwli@ciac.ac.cn; zysun@ciac.ac.cn

*To whom correspondence should be addressed

[†]Changchun Institute of Applied Chemistry

[‡]University of Science and Technology of China

The relationship between GB model and real system

The GB model used in this work is described in reduced units. Nevertheless, these model parameters can be mapped into real systems by rescaling all quantities with respect to suitable combinations of a characteristic length σ_0 , energy ϵ_0 , and mass m_0 . For example, for model molecular mapped ellipsoids with $\sigma_0 \sim 1nm$, $m_0 \sim 10^{-23}kg$, and $\epsilon_0 \sim 10^{-21}J$, the real time $\tau = \sigma_0(m_0/\epsilon_0)^{1/2}$ is approximately $10^{-10}s$. Moreover, the energy between a uniform aligning field and each ellipsoid is modelled by $U_i = E^*(\hat{e} \cdot \hat{u}_i)^2$, so the dimensionless intensity unit $E^* = 1$ approximately corresponds to $10^{-21}J$. Actually, such kind of mapping is only used for understanding the length scale and time scale of the present simulation, which cannot be used to quantitatively compare the simulation and the experimental results.

Structural and Dynamical Characterization of Liquid Crystal Structures

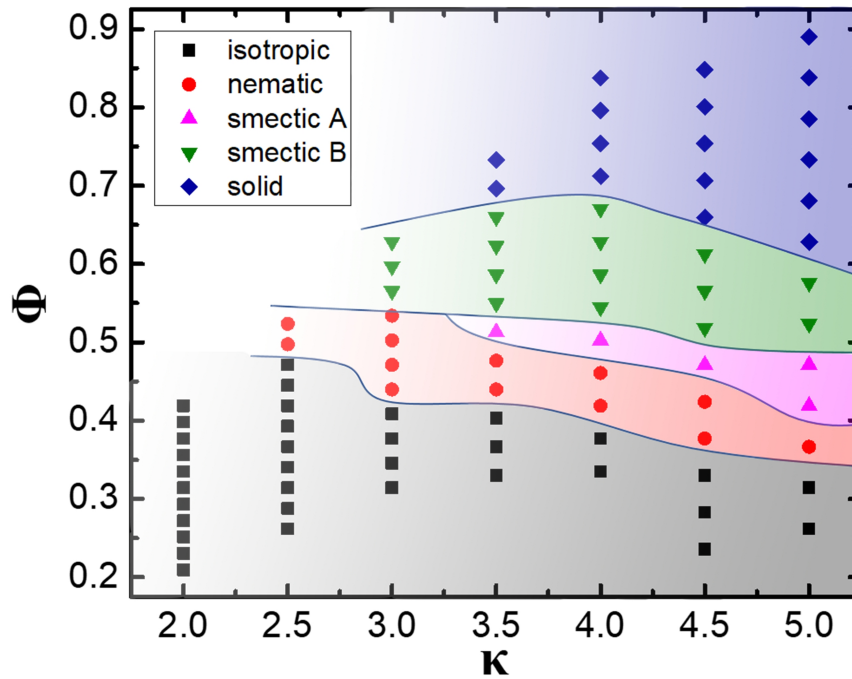


Figure S1: The structural diagram in $\phi - \epsilon$ plane in steady state, in which the solid lines are used to divide different phases. The volume of each ellipsoid is calculated by $V_i = \frac{4}{3}\pi\frac{a}{2}\frac{b}{2}\frac{c}{2} = \frac{1}{6}\pi\epsilon$. The number density $\rho = \frac{N}{V}$ (N is the number of the particles in the box and V is the volume of box). It is seen that the packing fraction is related to the aspect-ratio and the number density ($\phi = V_i N / V = \frac{1}{6}\pi\epsilon\rho$).

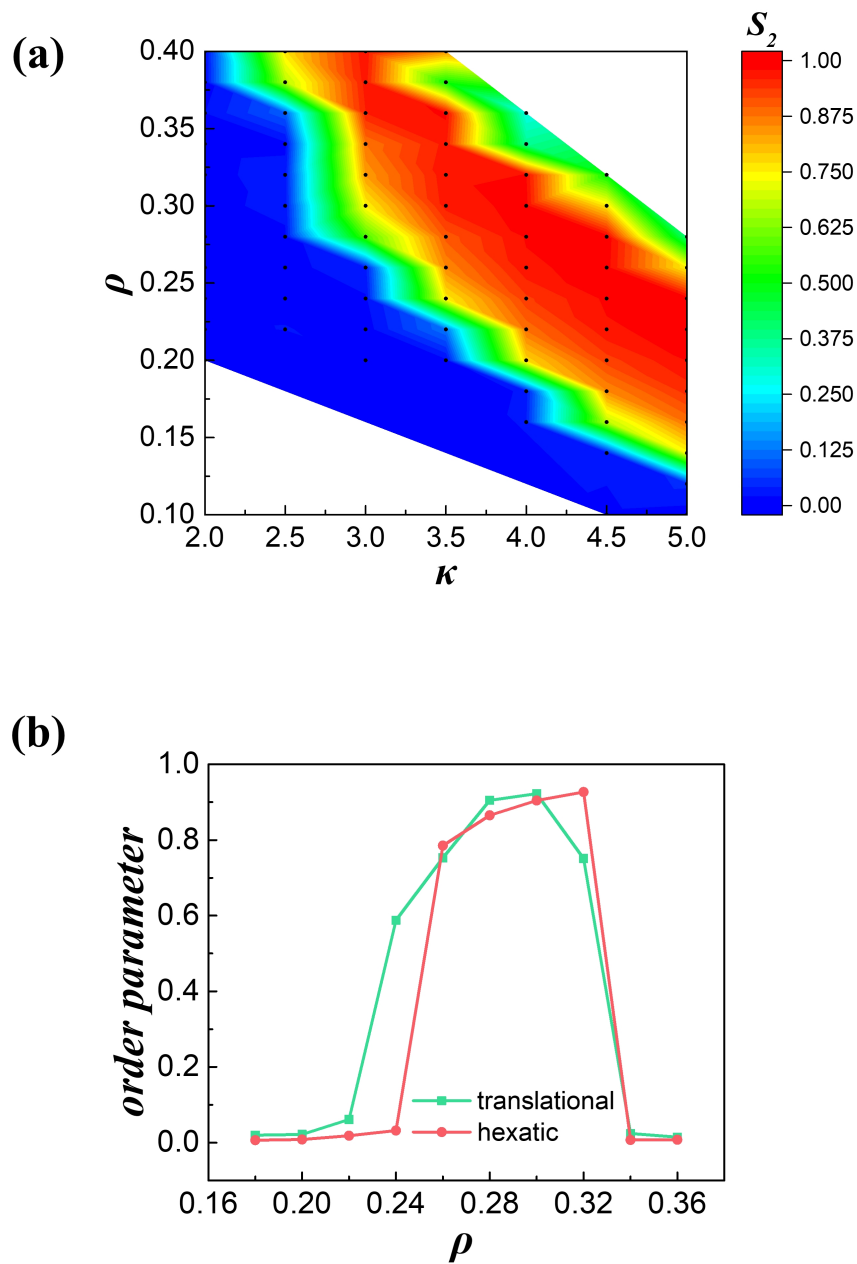


Figure S2: (a) The color map of the value of S_2 on the $\rho - \kappa$ plane corresponding to Fig.2(a), and the dark blue area represents isotropic phase. (b) The translational order parameter (green dot line) and hexatic order parameter (red dot line) line chart relative to the number density (ρ) at aspect ratio (κ) equal to 4.0. It can be seen that the density of 0.24 to 0.32 is the smectic phase, of which the density of 0.24 is the SmA phase, and the density of 0.26 to 0.32 is the SmB phase.

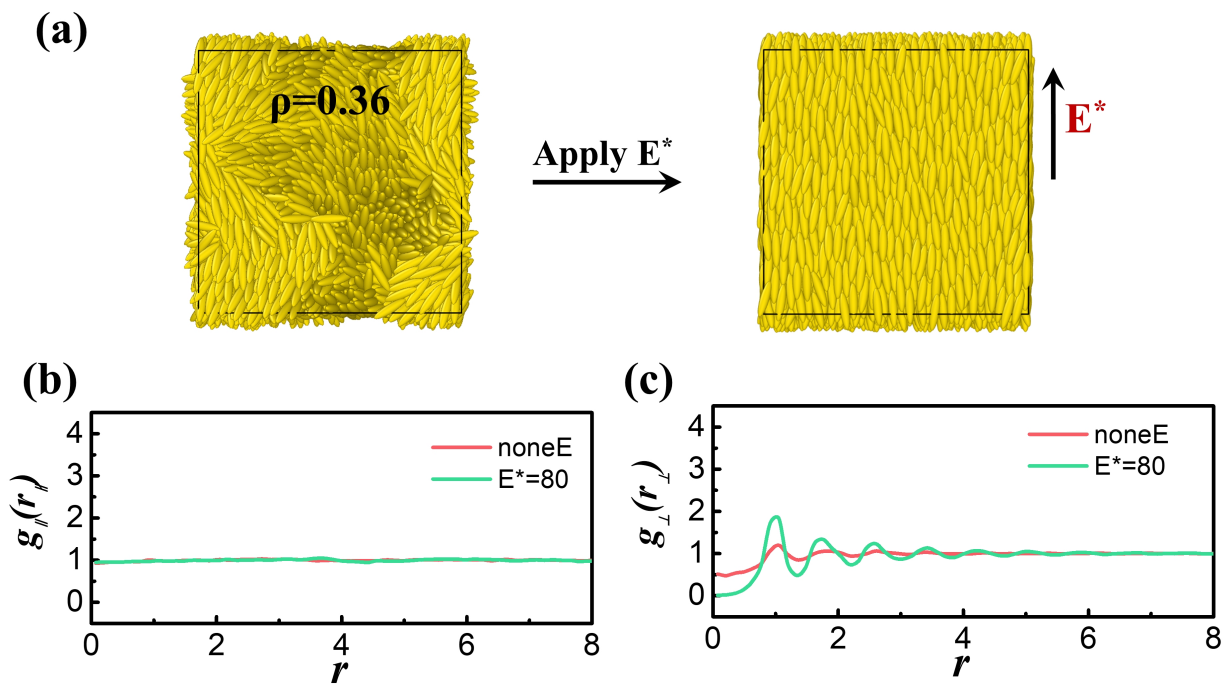


Figure S3: (a) The snapshots of solid in steady state (left) and under a constant electric field ($E^* = 80$). (b) and (c) are the parallel and perpendicular radial distribution functions $g_{\parallel}(r_{\parallel})$, respectively.

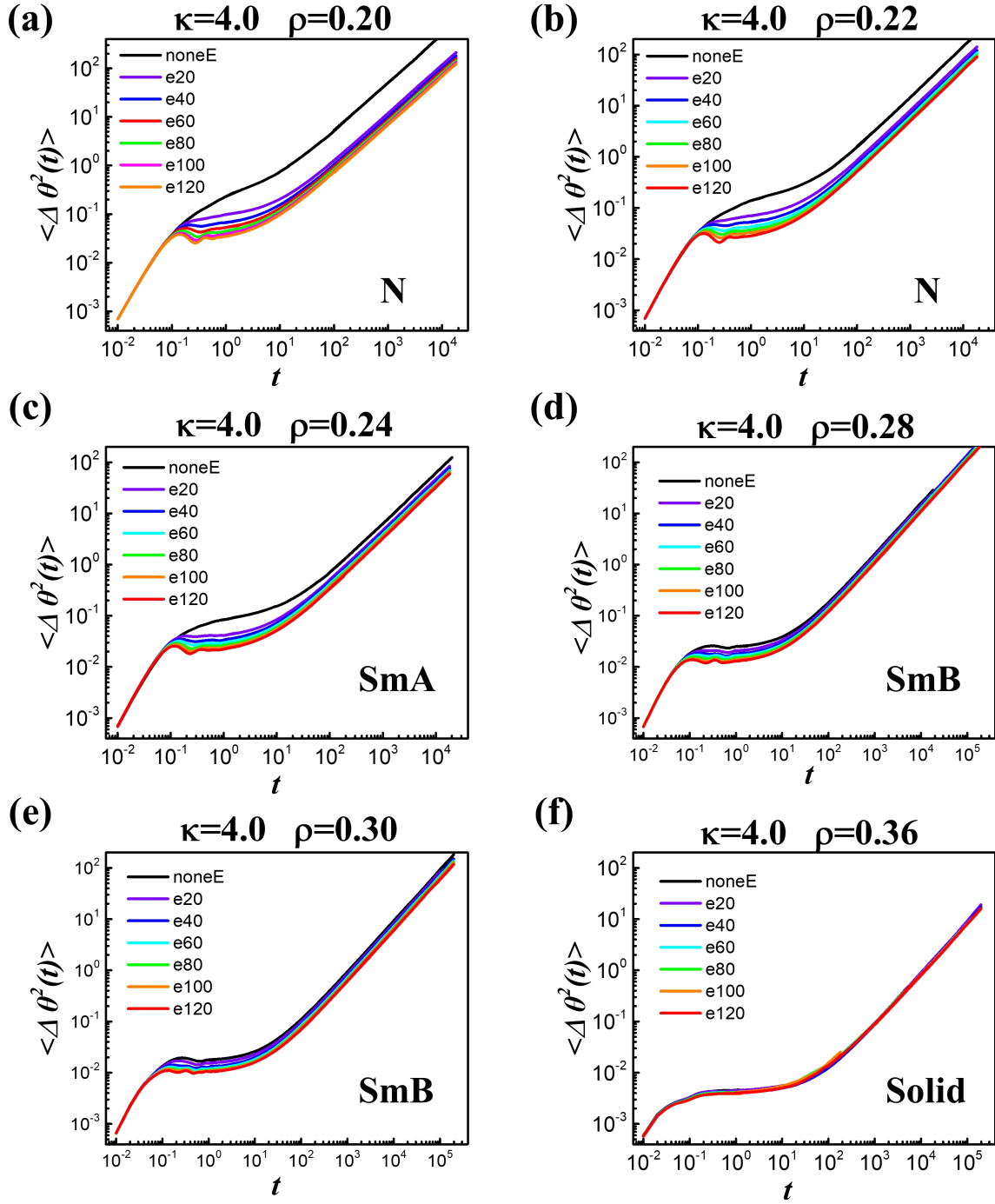


Figure S4: Mean-square angular displacement $\Delta r^2(t)$ of ellipsoids with $\kappa = 4.0$ at different number densities and different aligning field strength: (a)-(b) Nematic phase (N) at $\rho = 0.20, 0.22$, (c) Smectic-A phase (SmA) at $\rho = 0.24$, (d)-(e) Smectic-B phase (SmB) at $\rho = 0.28$, and 0.30 , (f) Solid phase at $\rho = 0.36$.

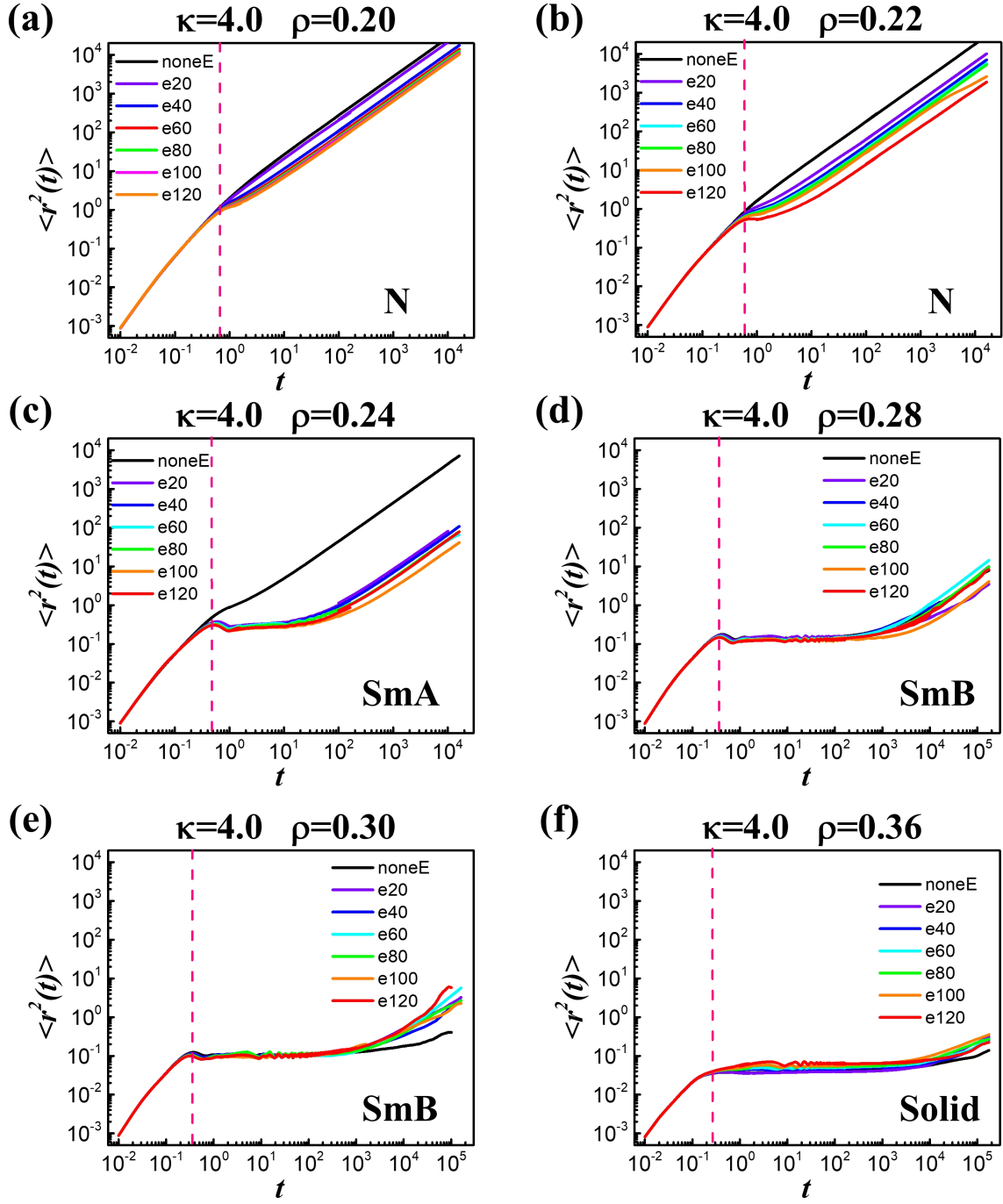


Figure S5: Mean-square displacement $\Delta r^2(t)$ of ellipsoids with $\kappa = 4.0$ at different number densities and different aligning field strength: (a)-(b) Nematic phase (N) at $\rho = 0.20, 0.22$, (c) Smectic-A phase (SmA) at $\rho = 0.24$, (d)-(e) Smectic-B phase (SmB) at $\rho = 0.28$, and 0.30 , (f) Solid phase at $\rho = 0.36$.

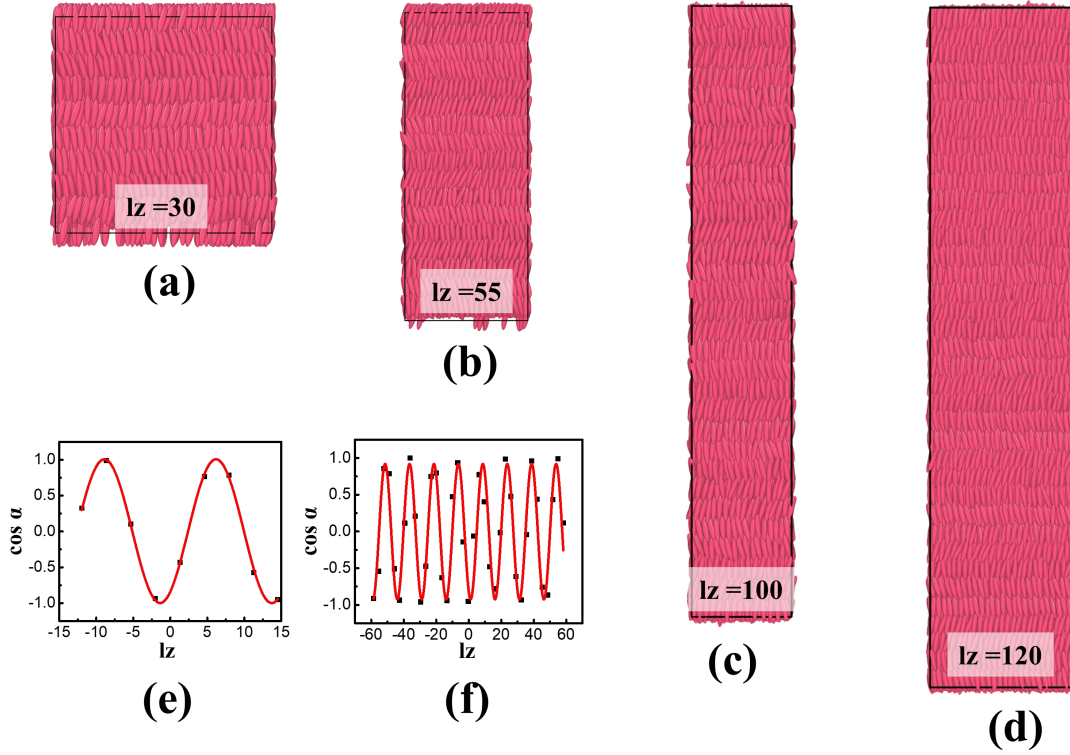


Figure S6: Typical snapshots of ellipsoids with shape anisotropy $\kappa = 4.0$ at number density $\rho = 0.30$ under external oscillating electric field $E^* = 100$, and *period* = 0.48: (a) 8000 particles in box with $L_x=L_y=L_z=30$, (b) 8000 particles in box with $L_x=L_y=22, L_z=55$, (c) 8000 particles in box with $L_x=L_y=16, L_z=100$, (d) 22500 particles in box with $L_x=L_y=25, L_z=120$, (e) twist angle profile $\cos\alpha(z) = \mathbf{n}(z) \cdot \mathbf{x}(z=0)$ corresponding to (a), (f) twist angle profile $\cos\alpha(z) = \mathbf{n}(z) \cdot \mathbf{x}(z=0)$ corresponding to (d). It is clearly seen that the chiral smectic phase is formed for systems with different box sizes, implying that the finite size effect can be neglected for the formation of chiral smectic phase.

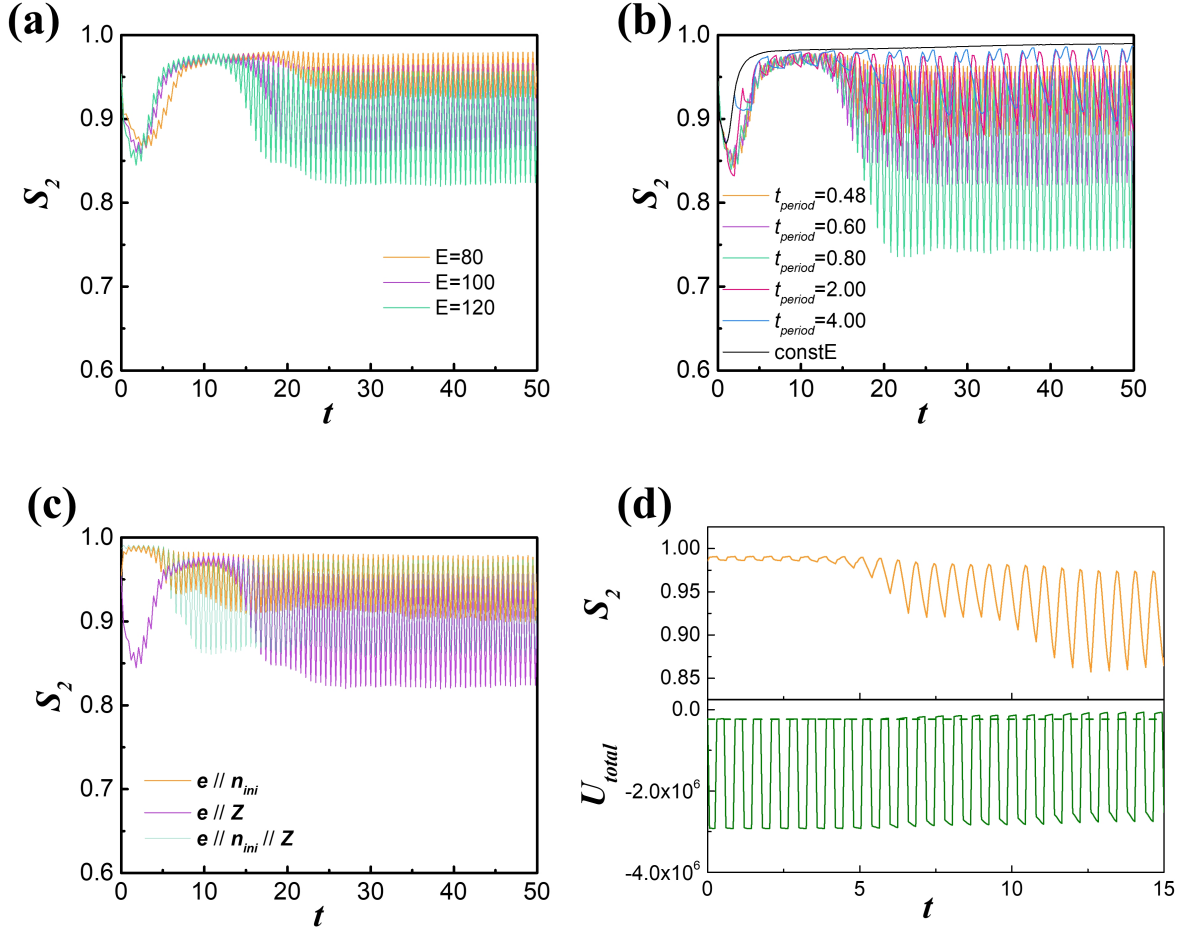


Figure S7: The order parameter(S_2) of system ($\kappa = 4.0$, $\rho = 0.30$) under the alternating external field with (a) fixed oscillating period ($t_{period} = 0.6$), and (b) fixed intensity($E^* = 120$). (c) The effect of the direction of the external field(\mathbf{e}) and the initial configuration(\mathbf{n}_{ini}) on the change of the order parameter(S_2) of the system($\kappa = 4.0$, $\rho = 0.30$, $t_{period} = 0.6$, $E^* = 120$). (d) The order parameter(S_2) and the total potential(U_{total}) of the system after adding the alternating external field. The green dotted line represents the energy of the system in the absence of the external field.

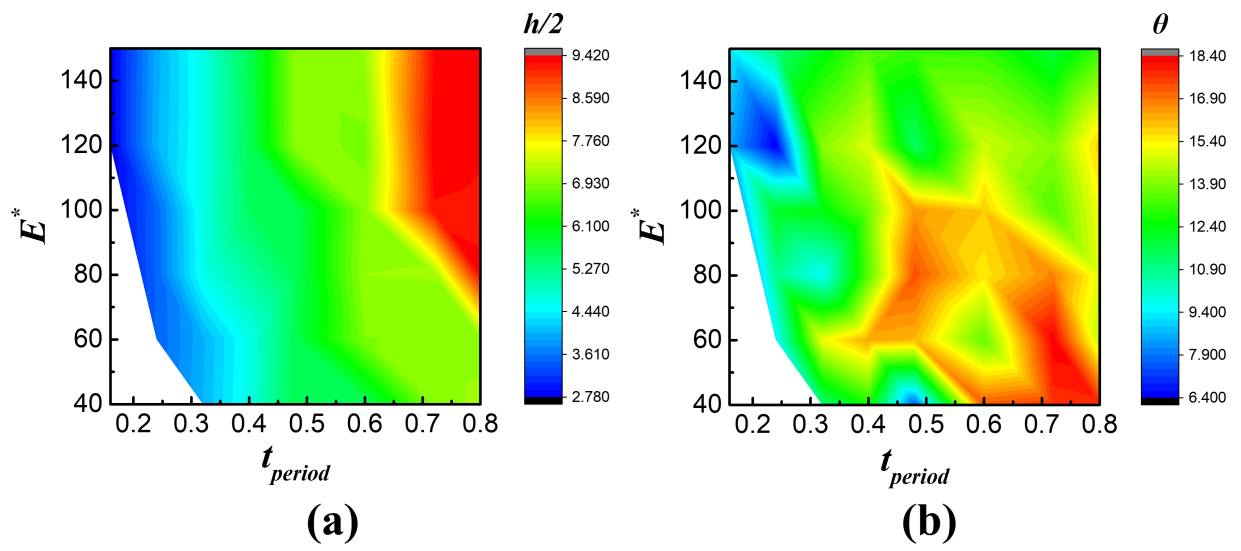


Figure S8: (a) The half-pitch of the chiral helix($h/2$) and (b) the tilt-angle(θ) in $E^* - t_{period}$ plane under the alternating field for ellipsoids with $\kappa = 3.0$, and $\rho = 0.40$.